10548 *Inorg. Chem.* **2009**, *48*, 10548–10552
DOI: 10.1021/ic901389v

Inorganic Chemistry
Article

Self-Template Synthesis of $CdIn_2O_4$ Hollow Spheres and Effects of Cd/In Molar Ratios on Its Morphologies

Jiaoxian Yu, Baibiao Huang,* Zeyan Wang, Xiaoyan Qin, Xiaoyang Zhang, and Peng Wang

State Key Laboratory of Crystal Materials, Shandong University, Jinan 250100, P. R. China

Received April 23, 2009

$CdIn_2O_4$ hollow spheres were synthesized by a self-template method. Cadmium nitrate ($Cd(NO_3)_2 \cdot 4H_2O$) and indium nitrate ($In(NO_3)_3 \cdot 4.5H_2O$) were used as raw materials. XRD and SEM were employed to characterize the structures and morphologies of as-grown samples. The effects of Cd/In ratios on the compositions, morphologies, and photocatalytic activities have been systematically investigated. A self-template growth mechanism of $CdIn_2O_4$ hollow spheres was proposed. And pure phase of $CdIn_2O_4$ can be obtained with Cd/In ratio of 1.3:2 annealing at 800 °C according to our experiments. The sample with the Cd/In ratio of 1.4:2 exhibited the highest photocatalytic efficiency, and more than 80% of Methylene Blue molecules can be decomposed in 180 min.

Introduction

$CdIn_2O_4$ is a well-known *n*-type semiconductor, which has been extensively studied as a gas sensor material.[1−7] The gas sensors fabricated based on $CdIn_2O_4$ have been proven to show a quick response and fast recovery to specific chemicals, such as Cl_2,[8] ethanol gas, etc., which was even better than the popular In_2O_3 and SnO_2 sensors.[9] However, there are still some problems in the synthesis of $CdIn_2O_4$ materials. Some impurity phases could easily appear, such as CdO and In_2O_3 phases, and it is very difficult to get a pure phase of $CdIn_2O_4$ materials.[10] Yang et al. reported that mixed phases of In_2O_3, CdO, and $CdIn_2O_4$ can be finally obtained, when they prepared $CdIn_2O_4$ using a direct current (DC) reactive magnetron sputtering method.[11] And some other authors also reported the similar results.[12] So investigations on the synthesis of pure phase $CdIn_2O_4$ is of great importance.

Recently, hollow spheres have attracted much attention due to its superior properties, such as large specific surface areas, less agglomerated configurations, efficient photocatalytic activities, technological applications including drug delivery and potential applications in electronics, optics, photonics, etc.[13−18] Up to now, two main processes, including template-directed synthesis and emulsion synthesis, are employed to synthesize the materials with hollow structure. And many materials of hollow sphere structure have been synthesized and investigated by the two kinds of processes, such as $Ni_{1-x}Pt_x$ hollow spheres,[19] CdS hollow spherical particles,[20] CdSe and TiO_2 hollow spheres,[21,22] necklacelike hollow carbon nanospheres,[23] Indium hollow spheres,[24] and $CaWO_4$ hollow microspheres,[25] etc. However, there is no

---

*To whom correspondence should be addressed. Tel: +86-531-8836-6324. Fax: +86-531-8836-5969. E-mail: bbhuang@sdu.edu.cn.

(1) Chu, X. F.; Liu, X. Q.; Song, Y. C.; Meng, G. Y. *Sens. Actuators B* **1999**, *61*, 19–22.
(2) Lou, X. D.; Shi, D. Y.; Liu, S. P.; Peng, C. Y. *Sens. Actuators B* **2007**, *123*, 114–119.
(3) Chu, X. F. *Mater. Res. Bull.* **2003**, *38*, 1705–1711.
(4) Dong, Y. F.; Wang, W. L.; Liao, K. J. *Sens. Actuators B* **2000**, *67*, 254–257.
(5) Babu, P. M.; Rao, G. V.; Uthanna, S. *Mater. Chem. Phys.* **2002**, *78*, 208–213.
(6) Mahanubhav, M. D.; Patil, L. A. *J. Cryst. Growth* **2006**, *297*, 411–418.
(7) San, H. S.; Li, B.; Feng, B. X.; He, Y. Y.; Chen, C. *Thin Solid Films* **2005**, *483*, 245–250.
(8) Mahanubhav, M. D.; Patil, L. A. *Sens. Actuators B* **2007**, *128*, 186–192.
(9) Cao, M. H.; Wang, Y. D.; Chen, T.; Antonietti, M.; Niederberger, M. *Chem. Mater.* **2008**, *20*, 5781–5786.
(10) Li, B.; Zeng, L.; Zhang, F. S. *Phys. Status. Solidi., A* **2004**, *201*, 960–966.
(11) Yang, F. F.; Fang, L.; Zhang, S. F.; Sun, J. S.; Xu, Q. T.; Wu, S. Y.; Dong, J. X.; Kong, C. Y. *Appl. Surf. Sci.* **2008**, *254*, 5481–5486.
(12) Chen, T.; Zhou, Z. L.; Wang, Y. D. *Sens. Actuators B* **2008**, *135*, 219–223.
(13) Holland, B. T.; Blanford, C. F.; Stein, A. *Science* **1998**, *281*, 538–540.
(14) An, K.; Kwon, S. G.; Park, M.; Na, H. B.; Baik, S.-I.; Yu, J. H.; Kim, D.; Son, J. S.; Kim, Y. W.; Song, I. C.; Moon, W. K.; Park, H. M.; Hyeon, T. *Nano Lett.* **2008**, *8*, 4252–4258.
(15) Yu, J. G.; Liu, W.; Yu, H. G. *Cryst. Growth Des.* **2008**, *8*, 930–934.
(16) Yu, J. G.; Yu, X. X.; Huang, B. B.; Zhang, X. Y.; Dai, Y. *Cryst. Growth Des.* **2009**, *9*, 1474–1480.
(17) Wang, P. H.; Pan, C. Y. *Colloid Polym. Sci.* **2000**, *278*, 245–249.
(18) Jeong, U.; Wang, Y. L.; Ibisate, M.; Xia, Y. N. *Adv. Funct. Mater.* **2005**, *15*, 1907–1921.
(19) Cheng, F. Y.; Ma, H.; Li, Y. M.; Chen, J. *Inorg. Chem.* **2007**, *46*, 788–794.
(20) Song, C. X.; Gu, G. H.; Lin, Y. S.; Wang, H.; Guo, Y.; Fu, X.; Hu, Z. S. *Mater. Res. Bull.* **2003**, *38*, 917–924.
(21) Zhang, X.; Xie, Y.; Xu, F.; Xu, D.; Liu, X. H. *Inorg. Chem. Commun.* **2004**, *7*, 417–419.
(22) Li, X. X.; Xiong, Y. J.; Li, Z. Q.; Xie, Y. *Inorg. Chem.* **2006**, *45*, 3493–3495.
(23) Wu, C. Z.; Zhu, X.; Ye, L. L.; OuYang, C. Z.; Hu, S. Q.; Lei, L. Y.; Xie, Y. *Inorg. Chem.* **2006**, *45*, 8543–8550.
(24) Zhang, Y. X.; Li, G. H.; Zhang, L. D. *Inorg. Chem. Commun.* **2004**, *7*, 344–346.

report on fabricating $CdIn_2O_4$ hollow spherical nanostructures by self-assembly template method.

In this work, we synthesized pure phase $CdIn_2O_4$ nanomaterials with hollow spherical morphologies by the self-assembly template method. The effects of the Cd/In ratios and annealing temperatures on the compositions and morphologies of $CdIn_2O_4$ composites were systematically investigated. A plausible growth mechanism of $CdIn_2O_4$ hollow spheres was proposed. And, the photocatalytic activities of the samples were also investigated.

Experimental Details

$CdIn_2O_4$ nanocomposites were synthesized by a self-template method in the experiments. Cadmium nitrate ($Cd(NO_3)_2 \cdot 4H_2O$), indium nitrate ($In(NO_3)_3 \cdot 4.5H_2O$), and critic acid of analytical reagent (AR) grade were employed as raw materials. And, the detailed experimental processes are as follows. First, $Cd(NO_3)_2 \cdot 3H_2O$ and $In(NO_3)_3 \cdot 4.5H_2O$ with different Cd/In molar ratios (i.e., 1:2, 1.1:2, 1.2:2, 1.3:2, and 1.4:2, respectively.) were dissolved into distilled water to form a clear solution. A proper amount of critic acid with the molar ratio of [Cd + In]/critic acid = 1:2 corresponding to the different Cd/In ratios in the starting materials were put into the above solution to get a sol solution. Then, the sol solution with pH value of ~1 was aged for 2 h before dried in an oven at 120 °C. The breadlike products were collected and ground to powders. Second, the powders were initially kept at 400 °C for 3 h to remove the organic reagents, and then kept at 800 °C for 3 h to accomplish the growth process. The oven was naturally cooled down to room temperature, and the samples were finally obtained.

In order to compare the catalytic properties of as-synthesized samples with the others, we prepared $CdIn_2O_4$(with starting Cd/In ratio of 1.3:2) through a chemical coprecipitation method previously reported by Chu et al.[26] as follows: First, $Cd(NO_3)_2 \cdot 3H_2O$ and $In(NO_3)_3 \cdot 4.5H_2O$ with a Cd/In ratio of 1.3:2 were dissolved into distilled water to form a clear solution. Then, NaOH solution, the coprecipitation agent, was added dropwise into the mixed solution until pH value reached 7−8. The precipitates were washed, filtered, dried, and ground before annealed at 800 °C.

The structures and morphologies of our samples were characterized by X-ray diffraction (XRD; Bruker AXS D8 advance powder X-ray diffractometer) and scanning electron microscopy (SEM; Hitachi S4800), respectively. Energy-dispersive spectroscopy (EDS) was employed to determine the final (after annealing) stoichiometry of Cd/In ratios in the samples. The Brunauer−Emmett−Teller (BET) surface areas were measured using a Builder 4200 instrument at liquid nitrogen temperature. And the pH value was determined by a PHSJ-3F pH detector.

The visible-light photocatalytic activities of as-synthesized samples were evaluated by the degradation of Methylene Blue (MB) aqueous solutions. This is recognized as one of the most standard methods for the evaluation of the catalytic activity.[27] In a typical photocatalytic experiment, 150 mg as-prepared samples were suspended in 50 mL MB aqueous solution with the initial concentration of 20 mg L^{-1} in the glass beakers. The pH value of the suspension was 5.7 determined by a PHSJ-3F pH detector. The suspension was kept in dark with continuously stirring for 3 h to get an adsorption−desorption equilibrium prior to irradiation. A 300 W Xe arc lamp (PLS-SXE300, Beijing Trusttech Co. Ltd.) with a 420 nm cutoff filter was used as the light source. And, 5 mL of aqueous suspension was collected every 30 min during the experiment. The photocatalytic efficiencies of our samples were evaluated by monitoring the dye decolorization at the maximum absorption around λ = 663 nm as a function of irradiation time in the separated MB solution with a UV−vis spectrophotometer (Shimadzu UV-2550).

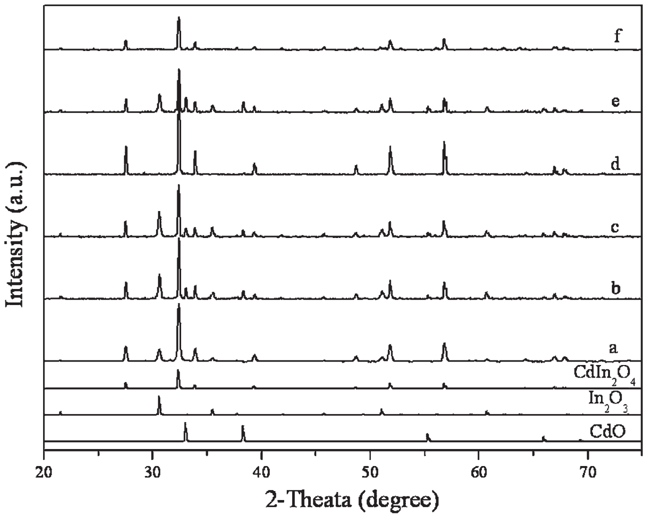

Figure 1. XRD patterns of the standard CdO, In_2O_3, $CdIn_2O_4$, and the as-prepared samples with different Cd/In ratios annealing at 800 °C (Cd/In ratios were adopted at (a) 1:2, (b) 1.1:2, (c) 1.2:2, (d) 1.3:2, and (e) 1.4:2) as well as the sample with starting Cd/In ratio of 1.3:2 prepared by a chemical coprecipitation method (f).

Results and Discussions

Figure 1 shows the XRD patterns of the as-prepared samples with different Cd/In molar ratios (i.e., 1:2, 1.1:2, 1.2:2, 1.3:2, and 1.4:2, respectively.) annealed at 800 °C. For comparison, standard CdO, In_2O_3, and $CdIn_2O_4$ patterns and the sample with a starting Cd/In ratio of 1.3:2 prepared by a chemical coprecipitation method are also presented. As shown in this figure, all the samples showed mixed phases of CdO, In_2O_3, and $CdIn_2O_4$, except for the sample with the starting Cd/In ratio of 1.3:2 (see Figure 1d and f). When, the Cd/In ratio is 1.3:2, $CdIn_2O_4$ is the only phase detected and no other phases can be traced, such as CdO, In_2O_3, etc. Chu et al. had reported that pure phase of $CdIn_2O_4$ can only be obtained when [Cd^{2+}] is higher or [In^{3+}] is lower than chemical stoichiometry in the starting materials.[26] This is totally consistent with our results.

SEM images of the samples with different Cd/In molar ratios were shown in Figure 2. The morphologies varied a lot from each other depending on the Cd/In molar ratios in the starting materials. When the ratio of Cd/In was stoichiometric (i.e., Cd/In = 1:2), the sample showed beanpod or peanutlike morphologies composed of very crystalline nanoparticles with sizes of about 100−150 nm, which can be clearly seen in Figure 2a. With the increase of the Cd/In molar ratios, the nanoparticles grew up and coupled together. Quadrangle or trigonal brackets were formed when the Cd/In was 1.1:2, and hollow structure was observed when the Cd/In ratio is 1.2:2 (Figure 2b and c). And, the numbers and sizes of hollow spheres increased constantly with the increase of Cd/In ratios. When the Cd/In ratio was 1.3:2 in the starting

---

(25) Wang, W. S.; Zhen, L.; Xu, C. Y.; Yang, L.; Shao, W. Z. *J. Phys. Chem. C* **2008**, *112*, 19390–19398.

(26) Chu, X. F.; Liu, X. Q.; Meng, G. Y. *Mater. Res. Bull.* **1999**, *34*, 693–700.

(27) Wang, Z. Y.; Huang, B. B.; Dai, Y.; Qin, X. Y.; Zhang, X. Y.; Wang, P.; Liu, H. X.; Yu, J. X. *J. Phys. Chem. C* **2009**, *113*, 4612–4617.

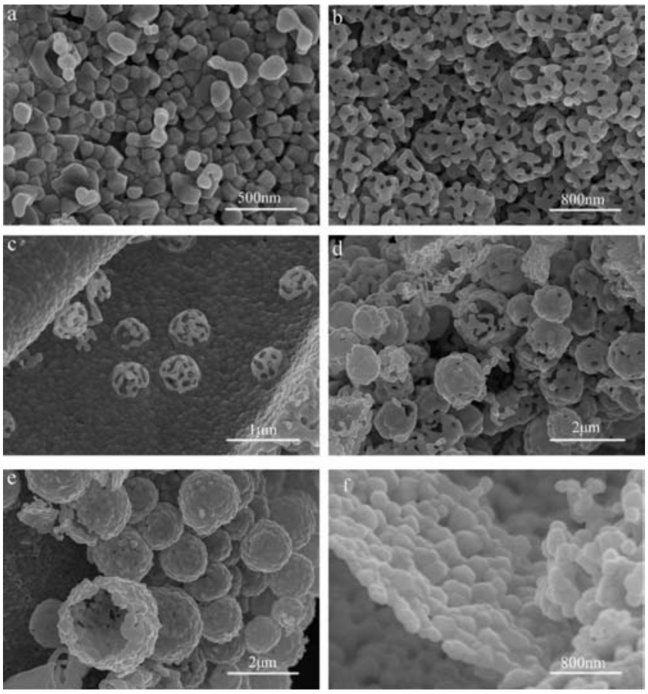

Figure 2. SEM images of the synthesized samples with different Cd/In ratios (Cd/In ratios: a = 1:2, b = 1.1:2, c = 1.2:2, d = 1.3:2, e = 1.4:2) and the sample with starting Cd/In ratio of 1.3:2 prepared by a chemical coprecipitation method (f).

Table 1. Actual Cd/In Ratios of As-Synthesized Samples

starting Cd/In ratio	1:2	1.1:2	1.2:2	1.3:2	1.4:2
actual Cd/In ratio	0.15:2	0.83:2	0.84:2	1.02:2	1.15:2

materials, only the hollow microspheres were observed (Figure 2d). And, according to the XRD pattern in Figure 1d, the hollow spheres are composed of pure phase $CdIn_2O_4$. The average diameter of the spheres is about 200 nm. The hollow spheres became larger and more integrated when the starting Cd/In ratio was 1.4:2. For comparison, Figure 2f presents the sample with starting Cd/In ratio of 1.3:2 prepared by chemical coprecipitation method. The sample, without any trace of hollow spheres, is composed of agglomerated particles. And, the average diameter of the particles could be estimated from Figure 2f to be about 250 nm.

The actual Cd/In ratios of the as-synthesized samples are listed in Table 1. As we can see, the actual Cd/In ratios in the products increased with the Cd/In ratios in the starting materials. The actual Cd/In ratios for the samples with the starting Cd/In ratios of 1:2, 1.1:2, 1.2:2, 1.3:2, and 1.4:2 are 0.15:2, 0.83:2, 0.84:2, 1.02:2, and 1.15:2, respectively. We can find that Cd may partly evaporate away when annealing at high temperature. Combine with the black powders of CdO on the lid of the crucible, we proposed that the hollow spheres could be formed by gaseous reactions in the experiments. The actual Cd/In ratio of 1.02:2 for initial Cd/In ratio of 1.3:2 was consistent with the XRD pattern showing the pure $CdIn_2O_4$ phase. The BET surface areas were measured thorough a Builder 4200 instrument at liquid nitrogen temperature. The BET surface areas for the samples with the starting Cd/In ratios of 1:2 and 1.3:2 are 13.78 and 22.06 m^2/g, respectively. The results showed that hollow sphere structures could effectively increase the BET surface areas. And in other words, the contact areas of catalytic reactions may be increased, which may further enhance the catalytic efficiency.

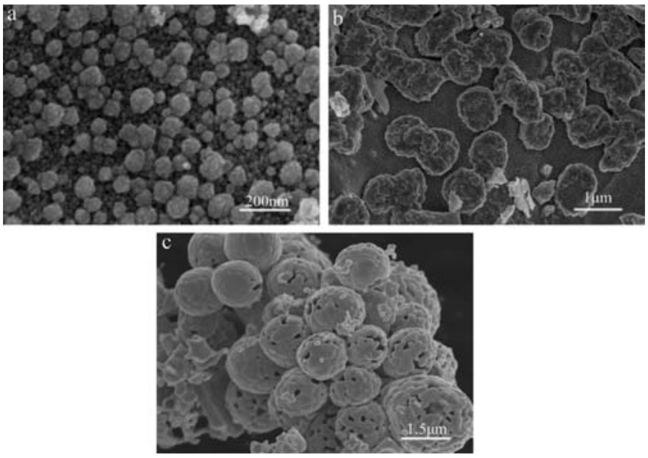

Figure 3. SEM images of the synthesized samples with Cd/In ratio of 1.3:2 annealing at (a) 400, (b) 600, (c) 800 °C for 3 h.

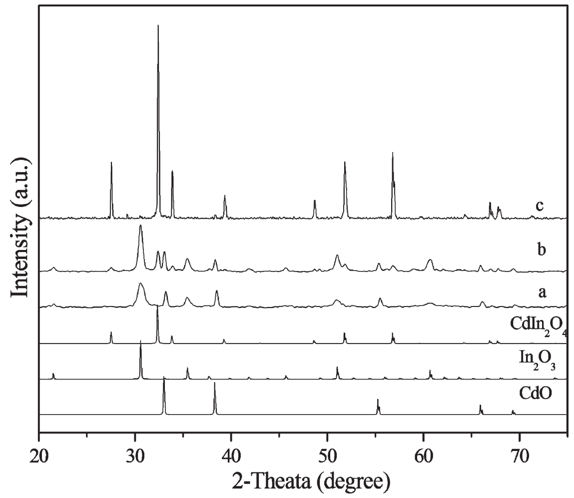

Figure 4. XRD patterns of the standard CdO, In_2O_3, $CdIn_2O_4$, and the synthesized samples with Cd/In ratios of 1.3:2 annealing at (a) 400, (b) 600, and (c) 800 °C.

In order to investigate the growth mechanism of the $CdIn_2O_4$ hollow spheres, the sample with Cd/In ratio of 1.3:2 was annealed at 400, 600, and 800 °C. SEM images and XRD patterns of the synthesized samples with Cd/In ratios of 1.3:2 annealed at different temperatures are shown in Figures 3 and 4, respectively. Figure 3a shows the SEM of the sample with Cd/In ratio of 1.3:2 annealed at 400 °C for 3 h. The sample showed a monodispersed spherical structure of about 60 nm agglomerated from some smaller nanoparticles, mainly composed of CdO and In_2O_3 according to the XRD pattern shown in Figure 4a. The size of these nanospheres grew up as the annealing temperature increased. The diameter of the spheres is about 1 μm for the sample calcined at 600 °C. $CdIn_2O_4$ hollow spheres with mean sizes of 1.5 μm were formed by annealing the precalcined samples at 800 °C for 3 h.

A plausible growth mechanism of $CdIn_2O_4$ hollow sphere composites can be elucidated according to the XRD and SEM analysis above, and the schematic illustration is shown in Figure 5. CdO and In_2O_3 nanoparticles were first formed and coupled together to form nanospheres when the samples

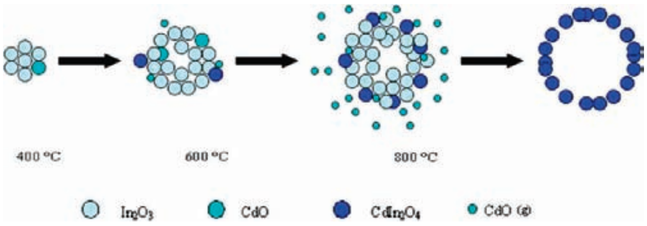

Figure 5. Schematic illustration of the growth mechanism of $CdIn_2O_4$ composite hollow spheres.

precalcined at 400 °C. The spheres behaved as templates in the following process of heat treatment, which played the same role as the rodlike Ga_2O_3 in the preparation of $NiGa_2O_4$ hollow rods.[28] More and more nanoparticles agglomerated on to the spheres with the increase of annealing temperature. And at the same time, the spheres and their constituent nanoparticles grew larger. Only small parts of CdO and In_2O_3 nanoparticles reacted with each other and transformed to $CdIn_2O_4$ phase when annealing at 600 °C. Most of the particles remained CdO and In_2O_3 phase (Figure 4 b), which may be due to the low annealing temperature. While the temperature increased to 800 °C, we found some black powders of CdO on the cover of the crucible in our experiments, which is probably formed by the evaporation of CdO. In_2O_3 nanobelts, by the evaporation of In_2O_3 powders, were synthesized when the temperature is as high as 1400 °C.[29] Hao et al. also reported that In_2O_3 nanowires were seldom formed when the temperatures were below 1350 °C, owing to its excessively low vapor pressure.[30] Meanwhile, CdO nanobelts can be synthesized by evaporating CdO powders at a comparatively lower temperature of about 1000 °C.[29] And, there is no Cd or other species that can be observed during the synthetic procedures. This indicates that the vapor pressure of CdO is higher than that of In_2O_3 and CdO is the dominant gaseous species in our experiments. Therefore, we think the inorganic reaction occurred as

$$CdO(g) + In_2O_3(s) \rightarrow CdIn_2O_4(s)$$

When CdO evaporated with the increase of annealing temperature, there is a CdO rich atmosphere in the crucible. On one hand, gaseous CdO reacted with In_2O_3 on the surface of the sphere to form $CdIn_2O_4$; on the other hand, In_2O_3 diffused outward to continue the reaction with CdO. In this way, $CdIn_2O_4$ hollow spheres were finally formed. This process is similar to the self-transformation process of the metastable aggregated particles.[31,32]

We learned from the reflectance spectrum that the samples could absorb visible light. Therefore, we investigated the catalytic activities of the samples under visible light. The photocatalytic activities of the series of our samples were evaluated by the bleaching of MB dye under the irradiation of visible light ($\lambda > 420$ nm). Figure 6 presents the photocatalytic activities of the synthesized samples. As we can see in this figure, the photocatalytic activities varied for the samples with different Cd/In ratios in the starting materials. The photocatalytic activity increased with the increase of Cd/In ratios. The sample with Cd/In ratio of 1.4:2 showed the highest photocatalytic activity, and more than 80% of MB molecules were decomposed in 180 min. With the starting Cd/In ratios of 1:2, 1.1:2, 1.2:2, 1.3:2, and 1.5:2, the fractions of the decomposed MB molecules in 180 min were 51%, 57%, 65%, 73%, and 43%, respectively. For pure CdO and In_2O_3 synthesized under identical conditions, 60% and 25% MB molecules were decomposed in 180 min, respectively. Comparing to CdO, the lower photocatalytic activities for Cd/In ratios of 1:2 and 1.1:2 may be mainly due to the existence of In_2O_3 and less $CdIn_2O_4$ hollow spheres. The higher photocatalytic activity of the sample with initial Cd/In ratio of 1.4:2 can be ascribed to the increase of $CdIn_2O_4$ hollow spheres. This may due to the unusual hierarchically nanoporous structure in hollow sample, which allows more effective transport for the reactant molecules to get to the active sites on the hollow shell.[15,33,34] In order to compare the catalytic properties of as-synthesized samples with the others, data of $CdIn_2O_4$ prepared through a chemical coprecipitation method were also presented in Figure 6. For this sample, 62% of MB molecules were decomposed in 180 min. This can further prove our views that the higher catalytic properties of our samples with starting Cd/In ratio of 1.3:2 and 1.4:2 can be ascribed to the hollow spheres.

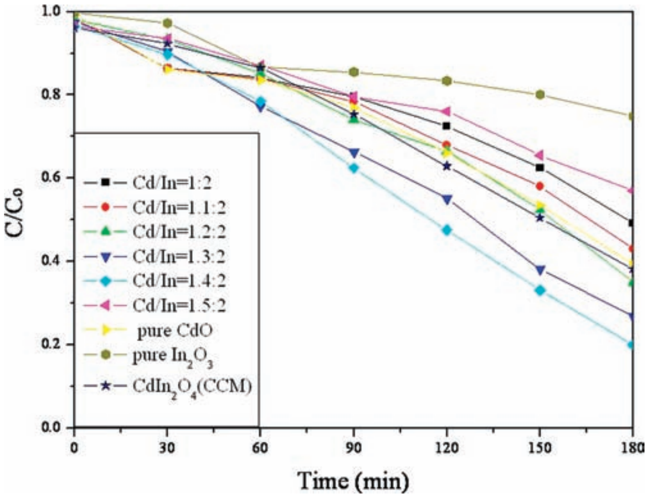

Figure 6. Concentration changes of MB as a function of irradiation time with CdO, In_2O_3, and the samples with different Cd/In ratios in the starting materials as well as $CdIn_2O_4$ prepared by a chemical coprecipitation method (CCM).

Conclusions

$CdIn_2O_4$ hollow spheres have been synthesized by the self-template method. The effects of Cd/In ratios on morphologies and visible-light photocatalytic activities have been systematically investigated. A pure phase of $CdIn_2O_4$ hollow spheres was obtained when the initial Cd/In ratio was 1.3/2. A plausible growth mechanism of $CdIn_2O_4$ hollow spheres depending on annealing temperatures was also proposed. Our results also showed that photocatalytic activity increased

---

(28) Xue, H.; Li, Z. H.; Ding, Z. X.; Wu, L.; Wang, X. X.; Fu, X. Z. *Cryst. Growth Des.* **2008**, *8*, 4511–4516.

(29) Pan, Z. W.; Dai, Z. R.; Wang, Z. L. *Science* **2001**, *291*, 1947–1949.

(30) Hao, Y. F.; Meng, G. W.; Ye, C. Y.; Zhang, L. D. *Cryst. Growth Des.* **2005**, *5*, 1617–1621.

(31) Yu, J. G.; Guo, H. T.; Davis, S. A.; Mann, S. *Adv. Funct. Mater.* **2006**, *16*, 2035–2041.

(32) Colfen, H.; Mann, S. *Angew. Chem., Int. Ed.* **2003**, *42*, 2350–2365.

(33) Wang, X. C.; Yu, J. C.; Ho, C. M.; Hou, Y. D.; Fu, X. Z. *Langmuir* **2005**, *21*, 2552–2559.

(34) Yu, J. G.; Su, Y. R.; Cheng, B. *Adv. Funct. Mater.* **2007**, *17*, 1984–1990.

with the increase of Cd/In ratios. The sample with an initial Cd/In ratio of 1.4:2 showed the highest photocatalytic efficiency in our experiments, and more than 80% MB molecules were decomposed under visible-light irradiation for 3 h.

Acknowledgment. This work was financially supported by the National Basic Research Program of China (No. 2007CB613302) and the National Natural Science Foundation of China (Nos. 20973102, 50721002 and 10774091).